Proceedings of the
Annual Stability Conference
Structural Stability Research Council
Denver, Colorado, March 22-25 2022

Exploring the effects of clip flexibility on the behavior of standing seam diaphragms to brace cold formed steel purlins

Michael W. Seek[1]

Abstract

Cold-formed steel C- and Z-shaped purlins in standing seam roof systems rely on the diaphragm action provided by the panels to restrain lateral movements and thus increase the load carrying capacity the purlins. The clip connection between the purlin and the panel has inherent and sometimes intentional flexibility designed to accommodate thermal deformations. The lateral deformation behavior of standing seam systems supported by Zees is highly nonlinear and this behavior is not well understood. The flexibility has major implications on the transfer of diaphragm forces throughout these systems and simplified models often grossly overpredict the demands on the diaphragm and the subsequent impacts on the purlin behavior. To investigate the behavior of standing seam diaphragm systems, shell finite element models are developed based on systems tested according to the AISI S908 Base Test. Initial models investigate separately flexibility in the panel versus flexibility in the purlin-to-panel clip connection to visualize the effects on the force transfer. Additional models were developed to investigate bi-linear behavior of the panels and clips. These models are calibrated to AISI S907 Cantilever Test data and then compared to base test data. The variation of the diaphragm forces relative to the various diaphragm configurations is presented.

1. Introduction

Standing seam roof panels used in conjunction with cold-formed steel purlins provide a very long lasting and economical solution to covering large areas under roof. The standing seam system consists of panels that are connected along their edges with a seam that is mechanically crimped. A standing seam clip, which provides a connection between the panels and the purlins, is crimped into this seam and then fastened to the purlin with self-tapping screws. The cold-formed steel purlins rely on the standing seam system to partially restrain lateral and rotational movement of the purlins which can greatly improve the global buckling strength of the purlins. This interaction between the purlin and the standing seam system is very complex and for the design of purlins in these systems, the industry in the United States has relied on the AISI S908 base test method (AISI 2017c). This test method requires a full-scale test of the purlin and standing seam panel system to determine a reduction factor that represents the reduced flexural capacity relative to flexural local buckling capacity of the globally restrained cross section.

[1] Associate Professor, Old Dominion University, <mseek@odu.edu>

While the AISI S908 test provides a good prediction of the strength of these systems, it has its limitations.

Therefore, there is an effort to develop analytical tools to make it possible to predict the behavior of these complex systems. These efforts have been aided by analysis tools such as CUFSM (Li and Schafer, 2010) which greatly improves our ability to analyze complex shapes and cross section stresses. Both Moen (2020) and Seek (2018) have developed analysis methodologies that have shown good correlation to tests performed according to AISI S908. In each of these methodologies, care must be taken to accurately predict the biaxial bending and torsion effects on the cross section. These effects are greatly influenced by the lateral and torsional restraint provided by the standing seam panels. The extent of these restraining effects can have a great impact on the flexural strength of the purlin.

To evaluate the rotational restraint provided by the panels to the purlin, designers can use a modified version of the test described in AISI S901 (AISI 2017a). Approximate values of the rotational stiffness of the common clip configurations as well as the effective standoff (effective height above the top flange of the purlin at which the lateral restraint of the panels) can be found in Seek et. al. (2021). The lateral restraint provided by the standing seam system is a function of the diaphragm stiffness. For cold formed panel systems, a cantilever test as described in AISI S907 (2017b) is used. The results of these cantilever tests for standing seam systems tend to be very non-linear. Although the tests are very non-linear, for the purpose of evaluating service load level deformations, the stiffness of the diaphragm is determined by a secant modulus at 40% of the peak force in the test.

For the purpose of predicting the strength of the purlins partially restrained by this standing seam diaphragm, this secant modulus is too simplified. For the analysis methodology developed by Seek (2018), the data from several S908 base tests (Emde, 2010) was used to calibrate the model. These base tests were performed on a variety of purlin cross sections and spans: 8Z2.5x057 and 8Z2.5x100 spanning 27 feet; 10Z2.5x057 and 10Z2.5x100 spanning 30 feet. The analysis methodology assumes a linear diaphragm stiffness to predict the lateral deflection of the diaphragm. The thicker purlins tested required larger demands on the diaphragm and at failure had lateral deflections on the order of 6 inches. For the analytical model to match the lateral deflections the analysis required using lower diaphragm stiffness values for the thicker purlins than the thinner purlins, indicating that the nonlinear behavior of the diaphragm is definitely has an influence.

The goal of this research, therefore, is to investigate two major aspects of standing seam diaphragm behavior. The first aspect is the extent to which the flexibility of the diaphragm is a function of the deformation of the panel verses the deformation of the clips. Being able to quantify this difference is important for several reasons. First, by separating the behavior, as manufacturers move towards more analytical approaches having an understanding of the dominating behavior will help in simplifying the analytical procedures. Second, the distribution of forces in the diaphragm depend on whether the flexibility is in the panel or the clips. Analytical models predict much larger shear demands in the clips near external anchor locations when the flexibility is in the panel versus the clips. The need to consider these large predicted

shear demands in design is controversial since in typical roof systems failures are not seen at these locations.

The second major aspect is to understand the extent to which the nonlinearity of the diaphragm needs to be included in the analysis. Clearly, the non-linear behavior of the diaphragm comes into play for systems tested according to AISI S908. The greater the demands on the diaphragm, the more flexible it becomes. Performing a nonlinear analysis adds a level of complexity to the analysis, so is it reasonable to approximate the stiffness of the diaphragm as linear once the nonlinear relationship between the demand and flexibility of the diaphragm is understood?

To accomplish this, a series of shell finite element models are constructed to investigate the forces interacting between the purlins and the panels. The models are created based on the tests on 8 in. deep Zees reported by Emde (2010). The first set of finite element models was designed to investigate the changes in diaphragm forces between the panels and purlins when the flexibility of the diaphragm is derived from pure shear deformation in the panels versus flexibility in the clip connection between the purlins and the sheathing. In this initial set of models, the panels and purlin to panel connections were modeled as linear-elastic.

It is clear with these systems that as the shear demand increases, the flexibility also increases so nonlinear behavior comes into play. Therefore for the second set of finite element models, the diaphragm was modeled as bi-linear. To approximate this bilinear behavior, AISI s90x cantilever test data was obtained for the standing seam system. A finite element model based on this data was constructed and the bi-linear diaphragm model properties were calibrated to this data. Similar to the linear models, for these bilinear models they were modeled separately with the flexibility of the diaphragm derived either from the shear deformation of the panels or the flexibility of the connection between the panel and the sheathing.

2 Basic diaphragm behavior

The behavior of Zee purlins interacting with the diaphragm is complex and in some ways counterintuitive. In the AISI S908 test, the system is tested in a flat roof condition; that is the pressure is applied perpendicular to the panels and parallel to the web of the Zee. Because of the rotated principal axes of the Zee, as this vertical load is applied parallel to the web, the Zee will deflect laterally in the direction perpendicular to the web. To facilitate analysis of Zee sections with rotated principal axes, Zetlin and Winter (1955) introduced the concept of modified moments of inertia and fictitious horizontal forces for analyzing a set of axes rotated from the principal axes. For a set of x and y axes rotated from the x' and y' principal axes, the modified moments of inertia about these axes are

$$I_{mx} = \frac{I_x I_y - I_{xy}^2}{I_y} \tag{1}$$

$$I_{my} = \frac{I_x I_y - I_{xy}^2}{I_x} \tag{2}$$

For a simple span Zee with length, L, subject to a uniform load, w, parallel to its y-axis, to calculate the lateral unrestrained deflection, Zetlin and Winter used a fictious horizontal force with a magnitude of $w(I_{xy}/I_x)$ as a driver for the lateral deflection. Incorporating the modified moments of inertia, the lateral deflection in the x-direction can be calculated by

$$\Delta_x = \frac{5\left(w\frac{I_{xy}}{I_x}\right)L^4}{384EI_{my}} \tag{3}$$

It is important to keep in mind that the fictitious force $w(I_{xy}/I_x)$ is just that, fictitious, and there is no net force applied in the x-direction. The deflection, Δ_x, is the maximum lateral deflection of the purlin when it is completely unrestrained laterally.

Next if we consider that the Zee has its top flange connected to a steel diaphragm, the diaphragm will restrict the lateral movement of the purlin. Assuming pure shear behavior in the diaphragm, as the purlin pushes on the diaphragm and the diaphragm restricts the movement, the interacting forces between Zee and diaphragm are essentially uniform along the length of the Zee. Ignoring any torsional rotation of the of the Zee, the magnitude of the uniform force acting in the diaphragm, w_{rest}, can be determined by considering displacement compatibility between the Zee and the diaphragm. In other words, by setting the net displacement of the purlin equal to the displacement of the diaphragm, the interacting force can be determined.

The net lateral deflection of the purlin is

$$\Delta_x = \frac{5\left(w\frac{I_{xy}}{I_x}\right)L^4}{384EI_{my}} - \frac{5w_{rest}L^4}{384EI_{my}} \tag{4}$$

The net lateral deflection of the diaphragm is

$$\Delta_x = \frac{w_{rest}L^2}{8G'd'} \tag{5}$$

The uniform restraining force in the diaphragm can be determined by equating the lateral deflection of the purlin to that of the diaphragm and solving for the uniform restraining force, w_{rest}.

$$w_{rest} = w\frac{\frac{5\left(\frac{I_{xy}}{I_x}\right)L^4}{384EI_{my}}}{\frac{5L^4}{384EI_{my}} + \frac{L^2}{8G'd'}} \tag{6}$$

For a given purlin, the uniform diaphragm force is dependent on the stiffness of the diaphragm. As the stiffness of the diaphragm approaches rigidity, ie G' is very large, the second term in the denominator approaches zero and the equation will reduce to

$$w_{rest} = w\frac{I_{xy}}{I_x} \tag{7}$$

Therefore, for a flat roof with anchors at the frame line, the maximum in plane force in the diaphragm is $w(I_{xy}/I_x)$. As the diaphragm becomes more flexible, the force in the diaphragm reduces. Logically, if the diaphragm has no stiffness, the force will reduce to zero.

It is important to remember that the uniform restraint force in the diaphragm in Eq. 6 is generated by unsymmetric bending. The fictitious force, $w(I_{xy}/I_x)$, is used to help quantify deflections using more conventional equations but ultimately there is no external lateral force applied to the diaphragm and thus the net force in the diaphragm must be balanced. As the force, w_{rest}, acts uniformly along the length of the Zee, the balancing force, P_{sc}, acting at the ends of the diaphragm is

$$P_{sc} = \frac{w_{rest}L}{2} \tag{8}$$

According to this theoretical model of diaphragm behavior, this balancing shear force, P_{sc}, can be large and is transferred between the Zee and the panels through a single clip connection at the very ends of the spans. By this theory, this force demand is often much larger than the capacity of the clip. The fact that failures are not seen at these locations either in AISI S908 tests or in installed roofs indicates that behavior is different than theorized.

In the above model of diaphragm behavior, it is assumed that the behavior is linear and the deformation of the diaphragm is totally a function of shear in the panels. As these two assumptions are changed, the distribution of the forces interacting between the purlin and the sheathing change.

3. Finite Element Models

3.1 Basic model configuration

Finite element models are developed according to tests performed by Emde (2010). Emde tested a range of purlins all with the same diaphragm configuration but with different bracing configurations. The finite element models presented here are based on two tests 8Z16A (8ZSx2.75x057) and 8Z12D (8ZSx2.75x100).

The tests were constructed with a pair of purlins spaced at 5 feet and spanning 27 feet. The panels were 7 feet long and cantilevered one foot beyond each purlin. The edges of the vacuum chamber were 6 inches beyond the end of the panel. Along the ends of the panels, an L1x1x1/8 was fastened with self-tapping screws to prevent the seams from opening at the ends. Torsion-only braces were applied at 10.5 feet from each end. Panels were attached to the purlins with low sliding clips with a ½ in. thermal block at the base of the clip.

The model was developed using SAP 2000. In the model, the global X axis was oriented along the span of the purlin, the global Y-axis in the opposite direction of gravity, and the Z-axis perpendicular to the web of the purlin. To model the purlin, the web is discretized into four elements along the height, the flange is discretized into three elements across the width and the flange stiffeners are modeled as a single element. Along the length of the purlin, it is discretized into 2 in. long elements. The resulting aspect ratio of the elements is typically slightly more than 2:1. The purlin elements are assigned the same thickness as the tested purlins and linear material properties with a modulus of elasticity of 29500 ksi.

The standing seam panels were discretized into 12 in. x 12 in. elements. The panel elements were connected to the purlin with 2 node link elements to represent the clips. The panel elements were assigned a membrane thickness of 0.0197 which is equivalent to the thickness of the panels. To match the effective standoff recommendations in Seek (2021), the panel was offset from the top flange of the purlin at a distance of 2.5 in. The orientation of the local axes of the panels and the panel to purlin link elements are provided in Table 1. The properties of these panel and clip link elements were varied as the different types of behavior of the standing seam system were simulated. The properties of these elements will be discussed in the corresponding sections.

Table 1: Panel and Panel Link Local Axes relative to Global axes

Global Axis	X	Y	Z
Orientation	Along purlin Span	Perpendicular to panel	Perpendicular to web
Panel Local Axis	x	z	y
Link Local Axis	z	x	y

The tests were performed with torsion-only braces, which as the name implies only prevents torsional rotation and does not restrict the lateral deflection of the purlin. To model these braces, a single frame element with the cross-sectional properties of a 6CS62.5x065 was used. A rigid 2-node link was used to connect the ends of the frame element to the web of the purlin at the intersection of the top and bottom flanges.

To model the rafter support conditions at the ends of the span, restraints were applied at a single node at the ends of the spans at the juncture of the web and bottom flange. The node was restrained against translation in the global Y and Z directions and against rotation about the global X-axis. To represent the anti-roll anchorage device that prevents torsional rotation of the end of the purlin, a single node at the intersection of the top flange and web was restrained in the global Z-direction.

One of the challenges in modelling the panels applied to the top flange is that the panels will try to act compositely with the purlins much like a steel beam topped with a concrete slab. In real systems, the panels are too flexible in the direction parallel to the span of the purlins to develop compressive stresses needed for composite action. To ensure that composite action doesn't occur in the models, two strategies were used. In some models, the translational stiffness of the link elements connecting the purlin to the panel is reduced to minimize the shear transfer and thus minimize the composite action. In other models, the axial stiffness of the panels in the direction parallel to the span of the purlin was arbitrarily reduced to minimize the composite action.

3.2 Linear diaphragm models

Initial finite element models investigated the diaphragm flexibility modeled as linear. The flexibility derived from a combination of shear deformation in the panels and the shear deformation of the clips connecting the panels to the purlins in the direction parallel to the panel seams (U2). To investigate this behavior, three models for each purlin cross section were developed. The first model (U2-rigid) treated the U2 shear deformation in the clip connections as rigid and thus all of the deformation of the in the diaphragm resulted from panel shear. The second and third model introduced flexibility in the clip U2 direction. Model designation U2-100 assigned an arbitrary stiffness of 100 lb/in in the U2 direction and model designation assigned an arbitrary stiffness of 50 lb/in in the U2 direction. The stiffness values assigned in all directions of the clip link elements for each model are shown in Table 2.

For each model, the diaphragm stiffness was adjusted so that the maximum lateral deflection in the model matched the modelled stiffness values reported by Seek (2018) which are based on the tested maximum deflection values at failure reported by Emde (2010). The peak pressure at failure, modeled diaphragm stiffness and corresponding panel shear modulus are given in Table 3. To model the variations in sheathing diaphragm stiffness, the panel elements are designated as orthotropic material and the shear modulus is adjusted. For the two material directions in the plane of the panels, the panel shear modulus, G, for a desired diaphragm shear stiffness, G', is

$$G = \frac{G'}{t} \tag{9}$$

Table 2: Link Element Properties

Model Series	U1 (lb/in)	U2 (lb/in)	U3 (lb/in)	R1 (lb-in/rad)	R2 (lb-in/rad)	R3 (lb-in/rad)
U2-rigid	10,000,000	10,000,000	1.	100.	1.	500
U2-100	10,000,000	100	1.	100.	1.	500
U2-50	10,000,000	50	1.	100.	1.	500

Table 3: Base test applied loads and deflections

Purlin	Designation	Link U2 stiffness (lb/in)	Max Pressure (psf)	Diaphragm stiffness, G' (lb/in)	Shear Modulus, G (lb/in^2)	Δ_{mid} Tested (in.)	Δ_{mid} Model (in.)
8Zx057	1A-Tested		17.68			1.86	
	U2-rigid	Rigid		230	11,675		2.13
	U2-100	100		460	23,350		2.14
	U2-50	50		3000	150,000		2.18
8Zx100	2D - Tested		37.65			6.17	
	U2-rigid	Rigid		110	5584		5.89
	U2-100	100		155	7868		5.91
	U2-50	50		230	11,675		5.91

The results of each model are shown compared to the theoretical model described in Section 2 in Figs. 1 and 2 for the 8Zx100 purlin and the 8Zx057 models respectively. Fig. 1(a) and Fig 2(a) display the forces transferred between the purlin and the panel at 1 foot intervals along the span. Fig. 2 (a) and 2 (b) show the unit shear (shear per foot depth of the diaphragm) for each model.

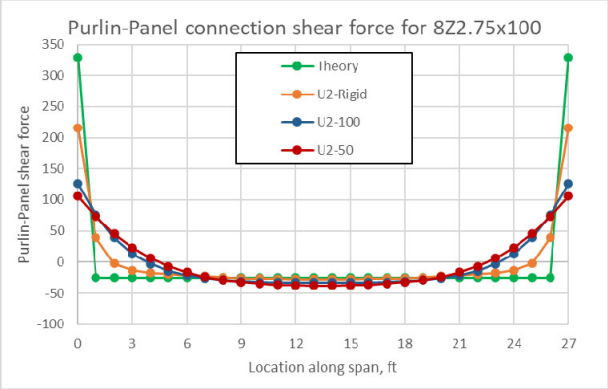

(a) Purlin to panel connection force

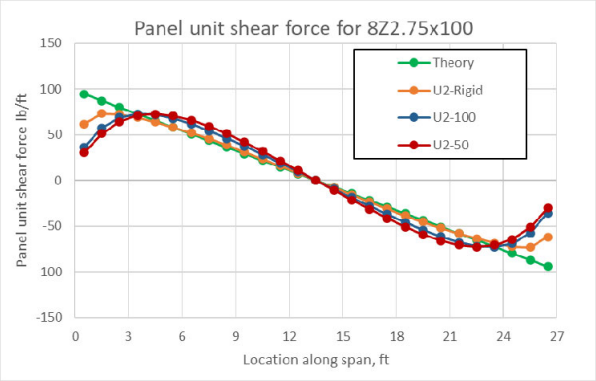

(b) Panel unit shear force

Figure 1 Analysis results for 8Z2.75x100

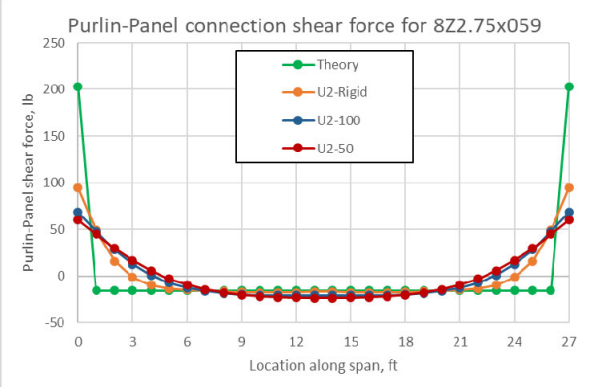

(a) Purlin to panel connection force

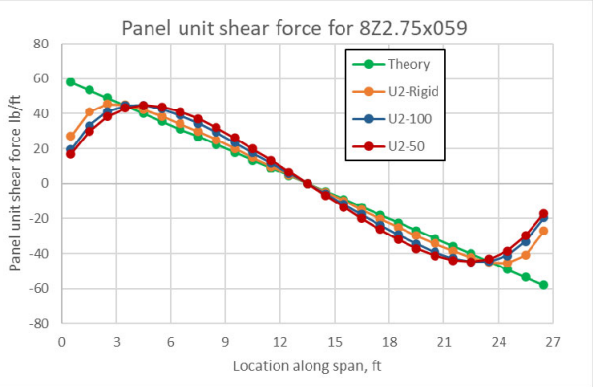

(b) Panel unit shear force

Figure 2 Analysis results for 8Z2.75x057

For these linear models, along the interior of the span, the uniform force corresponds well with the theory presented in Section 1. However, at the ends of the span, the theoretical model predicts a sharp reversal of the forces and the entire uniform force along the length is balanced at the very end of purlin with a magnitude, P_{sc} calculated by Eq. 8. The finite element models show that this balancing of forces at the end of the purlin occurs over a longer length at the end of the span. For the models where the flexibility is in modeled in the panels, the force reversal occurs over approximately 1/9 the span. For the models where the flexibility is in the clip connections, this reversal occurs over approximately 1/5 the span. Because of this longer region of force transition, the predicted peak force in the connection between the purlin and the panels is much less in the FE models than predicted by theory.

It is important to remember that the both the theoretical model and the finite element models were calibrated to the lateral deflection determined from the base test by varying the diaphragm stiffness of the standing seam system. If the goal is to move away from using the base test to predict the strength of purlin systems, this diaphragm stiffness must be known. The industry uses the cantilever test specified in AISI S907. For the standing seam system used in the base tests modeled herein, the results of the cantilever test of this system is shown in Fig. 3. There are two plots derived from this cantilever test. The first plot is the standing seam system tested "with no eave attachment" and the second plot is the system tested with the typical eave end conditions used in real installation. As can be seen from these plots, the addition of the eave attachment

adds considerable strength and stiffness. It can also be seen from the plots that the behavior of the standing seam system in shear is highly nonlinear. Note, the lateral deflection of purlins in a S908 base test is also nonlinear as can be seen in Figs. 5 and 6. From AISI S907, it is recommended that the stiffness of the diaphragm be taken as a secant modulus at 40% of the ultimate force in the diaphragm. This is shown in Fig. 3 for the system with no eave attachment and is calculated as a stiffness for G' of 467 lb/in. Also plotted relative to the cantilever test data is the calibrated stiffness of each of the base test models. For the 8Zx057 purlins, the calibrated linear stiffness is 230 lb/in. and for the 8Zx100 purlin the calibrated linear stiffness is 110 lb/in. Both of these trend lines were extended to the value of the peak unit shear predicted from the finite element models (45 lb/in for 8Zx057 and 73 lb/in for 8Zx100). These trendlines do not align well with the test data or each other for that matter. It is clear, therefore, that to predict the true lateral restraint provided by the standing seam system, the nonlinear nature of the diaphragm behavior must be considered.

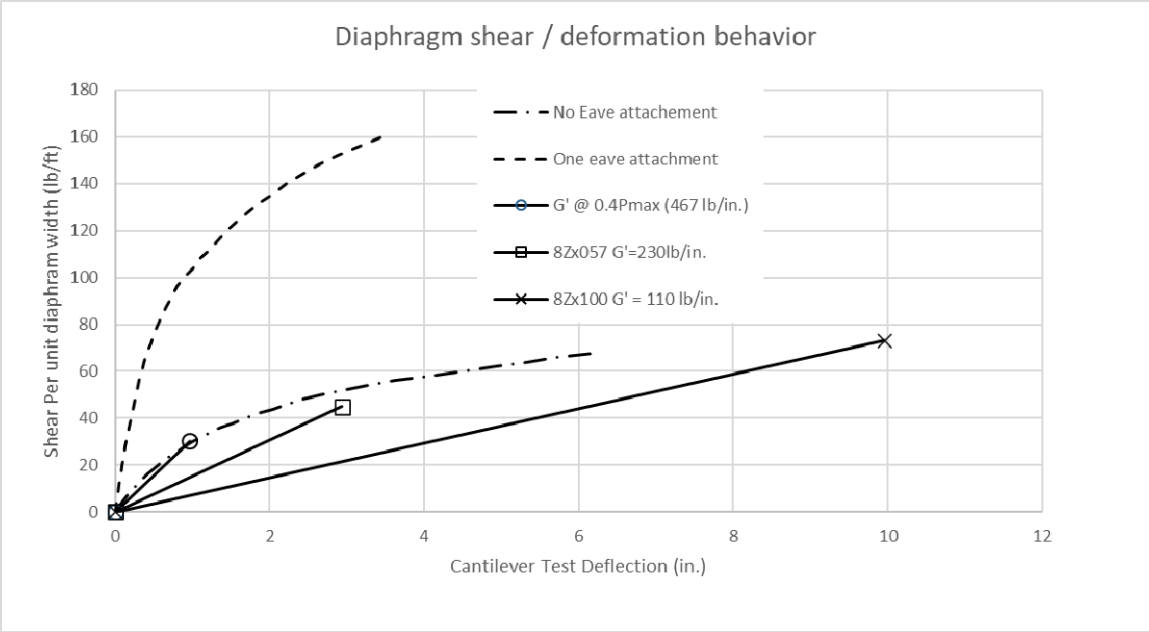

Figure 3 Comparison of AISI S907 test to linear stiffness approximations

3.3 Nonlinear finite element models

To test if the nonlinear behavior of the cantilever test can be replicated in a finite element model, and likewise, that nonlinear diaphragm behavior can better predict the stiffness of the diaphragm and lateral deflection in the AISI S908 base test, models were developed to incorporate material nonlinearity. Like the previous series of linear-elastic models, models were developed separately to investigate nonlinearity originating in the panels versus non-linearity in the purlin to panel clip connections. First, a FE model of the cantilever test was developed to isolate the diaphragm properties. One set of models investigated bi-linear properties of the panel in-plane shear (nonlin-panel) while the other set investigated bi-linear properties of the clip connection (nonlin-clip). These models were calibrated to the AISI S907 cantilever test data shown in Fig. 4. Because more detailed deformation data of the individual components was not available, these models were only compared to the overall force-deflection behavior obtained from the test with good correlation.

Once reasonable correlation between the FE models and the S907 cantilever test data was achieved, the non-linear properties of the diaphragm were applied to the FE models of the S908 base tests. With these models, the overall applied pressure-to-lateral-displacement behavior was compared to the test results with fair correlation. The forces between the panels and the purlins were extracted from the models and the behavior was compared to the theoretical model of the force interacting with the diaphragm.

3.3.1 Cantilever test models

To determine the properties of the standing seam system for modelling, a model of the S907 cantilever test was created. The overall test had dimensions of 10 feet wide by 15 feet deep. The purlins spanned 10 feet and there were 4 purlin lines spaced at 5 feet to give the 15 foot depth. The test frame and purlins were modeled as frame elements. The standing seam panels have a width and corresponding clip spacing of 2 feet. Two-node link elements were used to represent the clip connection between the panel and the purlin and these connections were spaced at 2 foot intervals. The previous linear models used clip spacing intervals of 1 foot. Increasing the spacing to 2 feet is a more realistic representation and has a significant impact on the behavior.

The first set of these cantilever test models investigated non-linear flexibility derived solely from non-linear panel shear. The material to model the panel was modelled as isotropic due to software limitations. The material was modeled as bi-linear. The diaphragm was modeled with an initial stiffness, G' = 650 lb/in. and a corresponding model shear modulus, G = 33,000 psi. The modulus of elasticity corresponding to this shear modulus is E = 85,800 psi. First yield was set at a unit shear value of 50 lb/ft which for the panel with a thickness of 0.0197 in corresponds to a shear stress of 212 psi and a shear strain of .00641 in./in. The secondary stiffness of the panel post yield is 50 lb/in. With the software used, SAP 2000, the stress-strain behavior of the isotropic material is defined according to normal stresses. For a pure shear relationship, the shear yield stress is half of the normal yield stress and shear strain corresponds directly with normal strain. The properties of the diaphragm defined according to the normal stress strain relationship is shown Table 4

Table 4: Nonlinear Panel Material properties

Stress-Strain node	Normal Strain (in/in)	Normal Stress (lb/in)
1	-0.0833	-1010
2	-0.00641	-423
3	0	0
4	0.00641	423
5	0.0833	1010

The panels were defined as shell elements with non-linear behavior enabled only for in-plane shear. Because the defined modulus of elasticity of the material needed to be defined at a low value to provide the desired shear behavior, stiffness modifiers were applied to the panel normal and bending stiffness (450 and 7840 respectively). The link elements connecting the purlin to the panel were defined as essentially rigid against translation about all 3 axes. For rotation, the same properties as defined in Table 2 are used. The load-deflection behavior of the model compared to the diaphragm tested according to AISI S907 is shown in Fig 4.

The second model of the diaphragm (nonlin-link) was developed to investigate the nonlinear behavior originating in the clip connections between the panel and the sheathing. The same basic cantilever test model as used to calibrate the diaphragm. Only slight changes were made to the elements modeling the panels and the link connections between the panel and the purlin. The panels were modeled as linear shell elements with a standard steel material. The link connections between the panel and the purlin were given bi-linear properties in the U2 and U3 direction. Stiffness in all other directions was assigned linear with the same properties as shown in Table 2. For the model with nonlinear behavior in the panels, the behavior was easy to predict because shear is essentially uniform in the cantilever test. Conversely, the forces in the clip connections vary depending on the location and orientation. Therefore, an iterative approach was used to determine the properties of the link elements. For simplicity and because more detailed information of the deformation behavior of the clips is not known, the same clip stiffness values were applied for both the U2 and U3 directions. The bilinear stress strain values for the clips in the U2 and U3 direction are shown in Table 5

Table 5: Nonlinear link force-displacement relationship

Node Point	Displacement (in)	Force (lb)
1	-6.05	-282
2	-0.29	-103
3	0	0
4	0.29	103
5	6.05	282

The load-deflection behavior of the model compared to the diaphragm tested according to AISI S907 is shown in Fig. 4

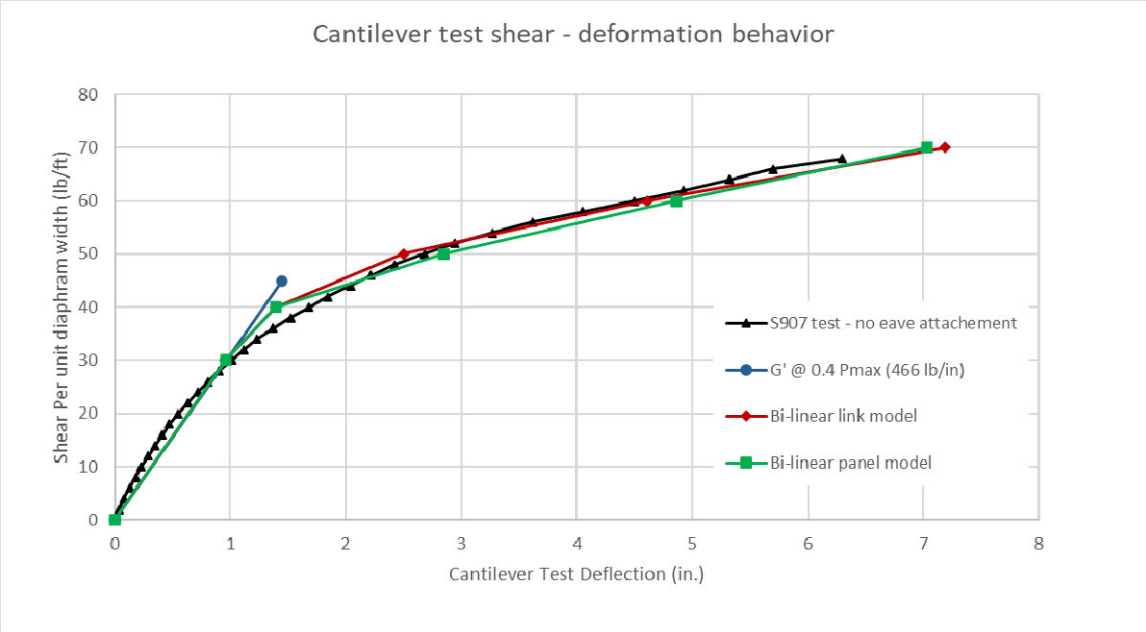

Figure 4: Comparison of FE models to AISI S907 test results

3.3.2 Base Test Models

The bi-linear diaphragm FE models that were calibrated to AISI S907 Cantilever test data as discussed in Section 3.3.1 were incorporated into the FE models of base tests. The models were set up with the same general model properties as discussed in section 3.1, with the exception of the changes to the diaphragm properties. Another major change was the spacing of the clips. The spacing of the clips was changed from 12 in. to 24 in. to match the width of the panels. The spacing of the clips was made symmetric about mid-span. Because the span length of the specimens tested according to the AISI S908 base test is an odd number (27 feet), this left 6 in. at the ends of the span between the last clip and the support location. This is common in the AISI S908 test and a partial panel is used at the end of the span to fully enclose the chamber. This small distance between the end of the span and the first clip does have an impact on the flexibility of the diaphragm.

To evaluate the FE models, the lateral deflection at the mid-span of the purlin in the models was compared to the test results as shown in Figs. 5 and 6.

Given the known variabilities in standing seam systems, the correlation between the lateral deflection of the tested system versus the finite element model is fair. For the models with the 8Zx057purlin, the models do not capture the initial stiffness but come close to predicting the behavior at the ultimate pressures. For the models of the thicker 8Zx100 purlin, the FE models align better with the test data throughout the range of motion but come up short at the ultimate pressures. Because the forces in the diaphragm are a function of this lateral displacement, it is important to get as close as possible to the displacement at ultimate load.

Figure 5: Comparison of lateral deflection for 8Z100 - AISI S908 test versus FE Model

Figure 6: Comparison of lateral deflection for 8Z100 - AISI S908 test versus FE Model

Although the correlation between the FE models and the test data is not perfect, it represents a step in the right direction. The predicted load-deflection behavior of the bi-linear models is much closer to the actual behavior than with a simple linear model. The models were created based on assumed properties calibrated to overall behavior of the diaphragm. With more detailed load-displacement data of the panels and clips themselves it is believed that correlation can be improved.

The shear forces in the clips connecting the purlin to the panels from the FE models are compared in Figs. 7 and 8. In general, the forces along the length of the span exceed those predicted by the theoretical model. However, at the ends of the spans where the greatest force demands are, the theoretical model lines up well with the force predicted by the bi-linear panel model. For the bi-linear clip link model, the predicted shear force is considerably less. It should also be noted that the force transfer behavior of the models for the 8Zx057 purlins is much closer to that in the linear models discussed in Section 3.2. This is to be expected because the force demands on the diaphragm from this thinner purlin are less and the diaphragm is just beginning to exhibit some nonlinearity. For the 8Zx100 purlins, the demands on the diaphragm are much higher and the nonlinear behavior is more evident.

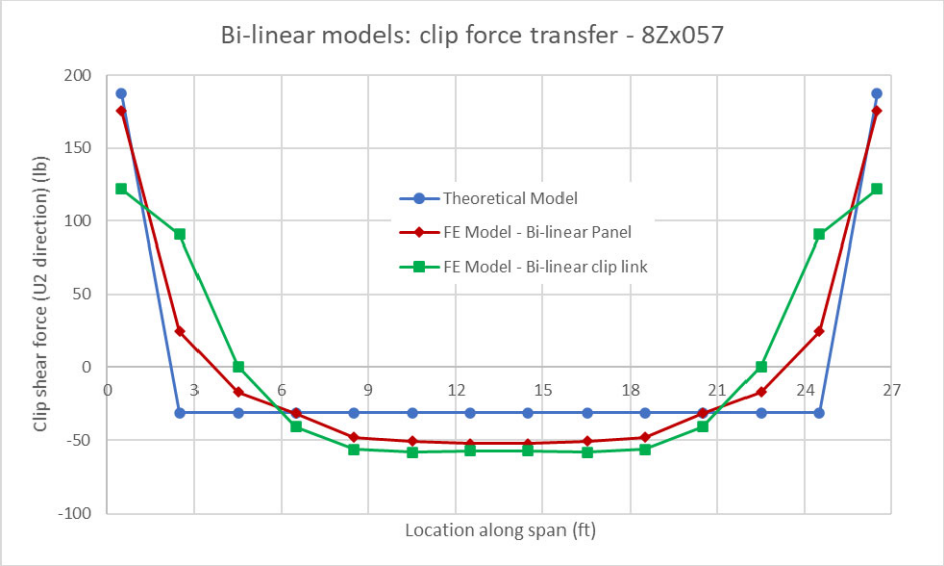

Figure 7: Force transfer between purlin and clip – 8Zx057

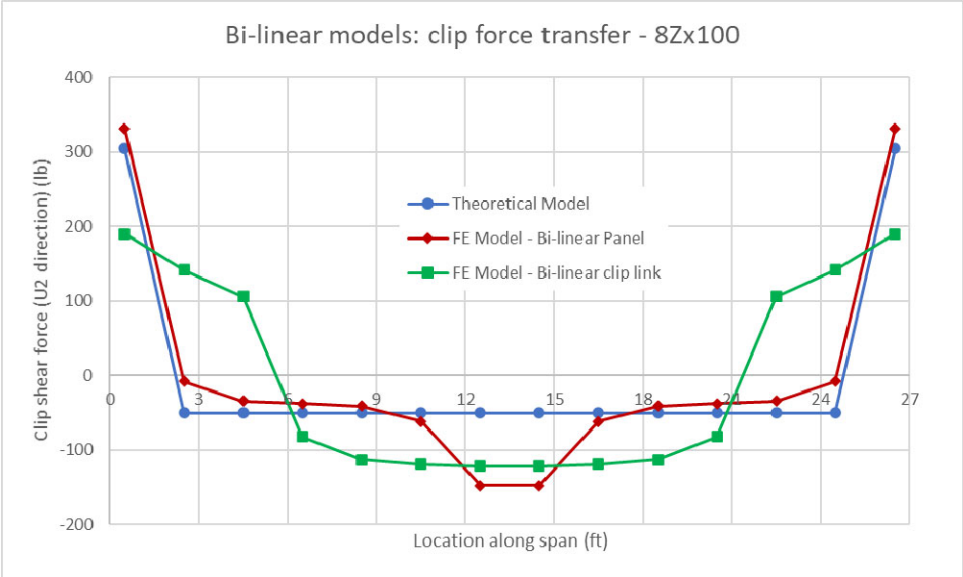

Figure 8: Force transfer between purlin and clip – 8Zx100

The unit shear force in the diaphragm was also derived from the shear forces in the clips and is shown in Figs. 9 and 10. The change in the distribution of shear forces in the clips at the ends of the spans of the purlins is reflected in the change in the shear distribution relative to the theoretical model. For the bilinear models, the maximum shear in the panels occurs at 3 to 5 feet from the end of the span. The magnitude of the shear force for both bi-linear cases equals or exceeds the magnitude from the theoretical model. Recognizing this small change is important for refining the theoretical model.

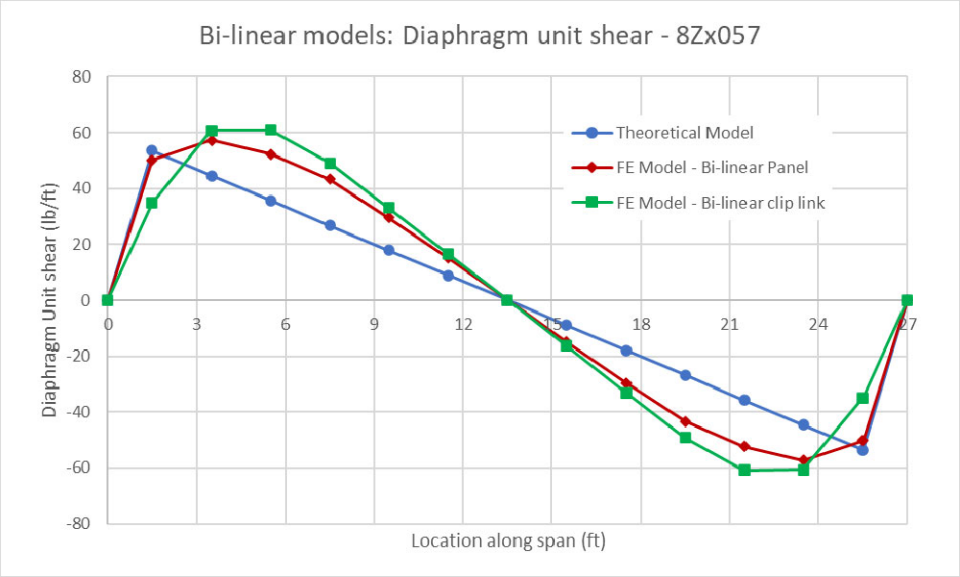

Figure 9: Diaphragm unit shear force – 8Zx057

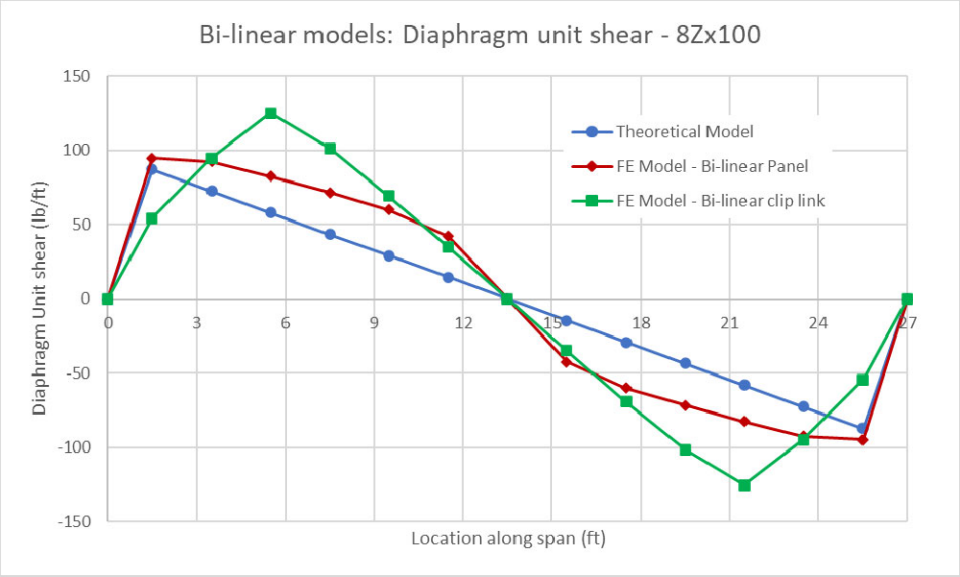

Figure 10: Diaphragm unit shear force – 8Zx100

4. Conclusions

Finite Element models were developed to investigate the transfer of forces through the clip connection of standing seam purlin systems supporting cold-formed Zees. The initial FE models defined the components of the standing seam system (clips and panels) as linear elastic and investigated the changes in behavior depending on whether the primary flexibility in the system was derived by the clip connections or the panel deformation. Both models showed that the reversal of forces at the ends of the spans occurs over a longer distance (1/10 of the span for systems with panel flexibility and 1/5 of the span for systems where flexibility is in the clips). Ultimately, by transferring this force over a longer distance, the maximum force that must be transferred by the clip is significantly reduced. Unfortunately, with these linear-elastic models,

because the diaphragm behavior of the panels is nonlinear and the forces interacting between the purlin and the sheathing are dependent upon the overall deformation of the system, to approximate the behavior with the model requires calibrating the stiffness to test data.

Additional finite element models were developed to determine first if modelling the standing seam system as bi-linear provided better correlation of the load-deformation behavior to AISI S908 test data and second to understand how these changes impact the transfer of forces between the purlins and the panels. Models were developed to investigate non-linear behavior originating either from the panel deformation or from deformation in the purlin to panel clip connection. Model bi-linear properties of the panels and the clip connections were determined by calibrating a model of S907 cantilever test assemblies to actual test data. These panel and clip properties were then applied to FE models of AISI S908 base test assemblies. The correlation of the applied-pressure-to-lateral-deflection behavior between the finite element models is fair for both diaphragm models. The correlation is much better than with models that define the diaphragm with linear behavior. Although the flexibility of the diaphragm was treated separately for panel deformation versus clip link deformation, it is likely that the real behavior is some combination of the two. By obtaining more detailed information on the nonlinear behavior of the individual clips and panels, better correlation can be likely obtained.

References

AISI (American Iron and Steel Institute) (2017a) S901-17 *Rotational-Lateral Stiffness Test Method for Beam-to-Panel Assemblies*. AISI. Washington, DC. 2017.

AISI (American Iron and Steel Institute) (2017b) S907-17 Test Standard for Determining the Strength and Stiffness of Cold-Formed Steel Diaphragms using the Cantilever Test Method. AISI. Washington, DC. 2017.

AISI (American Iron and Steel Institute) (2017c). S908-17 Base Test Method for Purlins Supporting a Standing Seam Roof System. AISI. Washington, DC. 2017.

Emde, M. G. (2010) Investigation of Torsional Bracing of Cold-Formed Steel Roofing Systems. Master's Thesis. University of Oklahoma. Norman, OK. 2010.

Li, A., Schafer, B.W. (2010) "Buckling analysis of cold-formed steel members with general boundary conditions using CUFSM: conventional and constrained finite strip methods." *Proceedings of the 20th International Specialty Conference on Cold-Formed Steel Structures.* 2010.

Moen, Cris (2020). "Structural Design Example – Four Span Metal Building Z-Purlin Line Supporting a Standing Seam Roof". Nextjournal https://nextjournal.com/runtosolve/metal-building-standing-seam-roof-design-example#design-specification.

Seek, M.W. (2018). "Flexural Strength of continuous-span Z-purlins with paired torsion braces using the Direct Strength Method". *Proceedings of the 24th International Specialty Conference on Cold-Formed Steel Structures.* 2018.

Seek, M. W., Avci, O and McLaughlin D (2021). Effective Standoff in Standing Seam Roof Systems. Journal of Constructional Research. V 180 May 2021.

Zetlin, L and G. Winter. (1955). "Unsymmetrical Bending of Beams with and without Lateral Bracing." Journal of the Structural Division, ASCE, Vol. 81, 1955.